

## Article

# Modeling the Effect of Alternative Cementitious Binders in Ultra-High-Performance Concrete

Solmoi Park <sup>1</sup> , Namkon Lee <sup>2</sup>, Gi-Hong An <sup>2</sup>, Kyeong-Taek Koh <sup>3</sup> and Gum-Sung Ryu <sup>2,\*</sup>

<sup>1</sup> Department of Civil Engineering, Pukyong National University, 45 Yongso-ro, Nam-gu, Busan 48513, Korea; solmoi.park@pknu.ac.kr

<sup>2</sup> Department of Structural Engineering Research, Korea Institute of Civil Engineering and Building Technology, 283 Goyangdae-ro, Ilsanseo-gu, Goyang-si 10223, Korea; nkleee@kict.re.kr (N.L.); agh0530@kict.re.kr (G.-H.A.)

<sup>3</sup> Korean Peninsula Infrastructure Special Committee, Korea Institute of Civil Engineering and Building Technology, 283 Goyangdae-ro, Ilsanseo-gu, Goyang-si 10223, Korea; ktgo@kict.re.kr

\* Correspondence: ryu0505@kict.re.kr

**Abstract:** The use of alternative cementitious binders is necessary for producing sustainable concrete. Herein, we study the effect of using alternative cementitious binders in ultra-high-performance concrete (UHPC) by calculating the phase assemblages of UHPC in which Portland cement is replaced with calcium aluminate cement, calcium sulfoaluminate cement, metakaolin or blast furnace slag. The calculation result shows that replacing Portland cement with calcium aluminate cement or calcium sulfoaluminate cement reduces the volume of C-S-H but increases the overall solid volume due to the formation of other phases, such as strätlingite or ettringite. The modeling result predicts that using calcium aluminate cement or calcium sulfoaluminate cement may require more water than it would for plain UHPC, while a similar or lower amount of water is needed for chemical reactions when using blast furnace slag or metakaolin.

**Keywords:** UHPC; thermodynamic modeling; phase assemblage; alternative cementitious binders; supplementary cementitious materials



**Citation:** Park, S.; Lee, N.; An, G.-H.; Koh, K.-T.; Ryu, G.-S. Modeling the Effect of Alternative Cementitious Binders in Ultra-High-Performance Concrete. *Materials* **2021**, *14*, 7333. <https://doi.org/10.3390/ma14237333>

Academic Editor: F. Pacheco Torgal

Received: 19 October 2021

Accepted: 22 November 2021

Published: 30 November 2021

**Publisher's Note:** MDPI stays neutral with regard to jurisdictional claims in published maps and institutional affiliations.



**Copyright:** © 2021 by the authors. Licensee MDPI, Basel, Switzerland. This article is an open access article distributed under the terms and conditions of the Creative Commons Attribution (CC BY) license (<https://creativecommons.org/licenses/by/4.0/>).

## 1. Introduction

Ultra-high-performance concrete (UHPC) is considered one of the most promising construction materials in terms of performance. It is typically produced at low water-to-binder ( $w/b$ ) ratios (0.15–0.25) and exhibits outstanding mechanical properties (compressive and tensile strengths exceeding 120 and 5 MPa after 28 days of curing) [1,2]. Due to the use of low  $w/b$  ratios, UHPC generally possesses extremely low porosity and excellent resistance to various chemical degradations. UHPC has been a topic of numerous studies which focused on various aspects of UHPC, such as its fresh and hardened state properties [3–7], effects of mix designs [8–11] and its performance at a structural level [12–15]. Due to the fact that the mixture proportioning and production methods of UHPC became mostly standardized in many countries, Portland cement (PC) is used as a cementitious binder along with silica fume in most cases. This is particularly important in recent years, where the high CO<sub>2</sub> footprint of PC has been a global concern and the demand for more sustainable cementitious binders is dramatically increasing.

Some attempts have been made to investigate the effect of using alternative cements or supplementary cementitious materials in the replacement of PC in UHPC. Song et al. [16] studied the effect of calcium sulfoaluminate cement (CSA) addition on the microstructure of UHPC, and showed that CSA tends to reduce the autogenous shrinkage of UHPC, concluding that a 5–15% addition is optimal. It is also reported that a denser matrix is formed when CSA is added to UHPC [16]. The use of calcium aluminate cement (CAC) as a cementitious binder in UHPC was intensively investigated by Lee et al. [17], who reported that CSA-based UHPC is capable of withstanding heat exposure and is free from spalling,

whereas typical UHPC is expected to completely lose its form at an exposure temperature  $\sim 400$  °C.

The effect of blast furnace slag (BFS) incorporation in UHPC can vary depending on the curing age. The incorporation of BFS in UHPC is generally known to decrease the compressive strength at early age (1–3 days) by 18–39% [18], while the strength can be higher in the BFS-containing UHPC in comparison with the plain one after 28 days [19,20]. The effect of BFS on the properties of UHPC can also vary depending on its replacement ratios. A study by Abdulkareem et al. [21] suggests that incorporation of BFS accelerates the hydration and refines the pore structure, while a high content of BFS may reduce the compressive strength by decreasing the amount of C-S-H in UHPC. The use of metakaolin (MK) in UHPC has been found to improve the early-age strength while decreasing the later-age strength [22]. The loss in the strength when MK is used to replace PC can be 11.8% relative to the strength of the control sample after 28 days of curing [22]. On the other hand, the use of very fine MK (so-called nano MK) is reported to increase the strength by 7.9% at the sample age of 28 days at a dosage as low as 1% [23]. Materials obtained from other sources can also be used to make UHPC (i.e., demolition waste [24], mine tailings [11], cement kiln dust, rice husk ash [25]) and achieve performance comparable to the ordinary system.

Despite an increasing number of studies having investigated the mechanical properties of UHPC incorporating cementitious binders other than PC, their microstructural information, which dictates the evolution of their properties, and performance is rarely available in the literature. Therefore, this study conducts thermodynamic simulations to predict the phase assemblages of UHPC in which PC is replaced with other cementitious binders, including CAC, CSA, MK or BFS.

## 2. Materials and Methods

The mix proportion of UHPC used in this work is shown in Table 1. The water-to-cement and water-to-binder ratios of the modeled UHPC were 0.2 and 0.16, respectively. The cement denotes PC, which was gradually replaced by either CAC, CSA, MK or BFS in the simulation. The compositions (Table 2) and reaction degrees of the binders reported in previous studies were used (PC [26], CAC [27], CSA [26], MK [28] and BFS [29]). The phase assemblages of UHPC mixtures incorporating PC, CAC, CSA, MK or BFS were predicted using GEM-Selektor v3.7 [30,31] and Cemdata18 [32].

**Table 1.** Mix proportion of UHPC.

Materials	Cement	Silica Fume	Silica Powder	Water
Mass Ratio	1.00	0.25	0.25	0.20

**Table 2.** Oxide compositions (mass-%) of raw materials obtained from other studies.

Oxides	PC [26]	CAC [27]	CSA [26]	MK [28]	BFS [29]
CaO	60.7	36.6	41.8		41.6
SiO <sub>2</sub>	20.6	4.1	8.5	52.0	36.6
Al <sub>2</sub> O <sub>3</sub>	5.0	40.3	30.4	43.8	12.2
Fe <sub>2</sub> O <sub>3</sub>	3.4	16.3	2.1	0.3	0.9
SO <sub>3</sub>	2.4	0.3	12.0	0.1	0.6
Na <sub>2</sub> O	0.2		0.1	0.3	0.2
K <sub>2</sub> O	1.0		0.3	0.1	0.3
MgO		0.1	2.2		7.1
SrO	0.1		0.1		
TiO <sub>2</sub>		1.8	1.5	1.5	
P <sub>2</sub> O <sub>5</sub>		0.2		0.2	
MnO					0.1

### 3. Results

#### 3.1. CAC-Containing UHPC

The predicted phase assemblage of UHPC containing CAC is shown in Figure 1. The phases which were predicted as stable in neat UHPC are C-S-H, ettringite, Fe-hydrogarnet and calcite. It is noted that portlandite was found to be unstable in all mixtures. Replacing PC with CAC in UHPC of up to 10% by mass resulted in the formation of more ettringite and Fe-hydrogarnet but reduced the amount of C-S-H and the overall volume of solid phases. The modeling result suggested that the overall volume of solid phases would increase when the replacement ratio is above 10%, due to the formation of strätlingite. The formation of strätlingite and the increase in the solid volume continued up to a 42% replacement ratio, where formation of  $\text{Al}(\text{OH})_3$  begins; the increase in the solid volume continues, but at a much lower rate, due to the gradual formation of  $\text{Al}(\text{OH})_3$  and the reduced strätlingite formation.

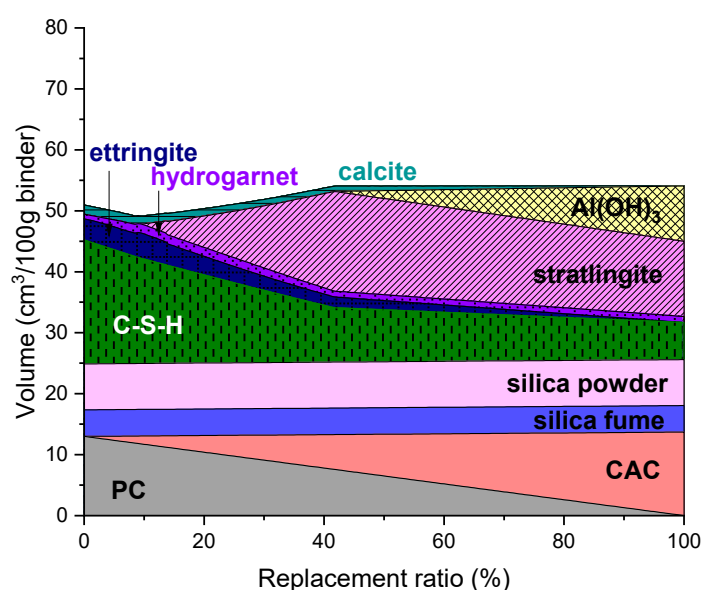


**Figure 1.** Predicted phase assemblage of UHPC containing CAC.

#### 3.2. CSA-Containing UHPC

The predicted phase assemblage of UHPC containing CSA is shown in Figure 2. The phases which are predicted as stable in the CSA-containing UHPC were similar in the case of the CAC-containing mixture, while their volumes varied. In general, the volume of ettringite was higher, and accordingly the volume of C-S-H was predicted to be lower in the CSA-containing UHPC. The formation of strätlingite and  $\text{Al}(\text{OH})_3$  in the CSA-containing UHPC was observed at similar replacement ratios that resulted in formation of those phases in the CAC-containing UHPC. The overall solid volume sharply increased at a 10% CSA replacement ratio, which coincides with the formation of strätlingite, similar to the CAC-containing UHPC. The increase in the solid volume continued even after the formation of  $\text{Al}(\text{OH})_3$  started in the CSA-containing UHPC, unlike the case of the CAC-containing UHPC, which can be associated with the continued formation of ettringite.

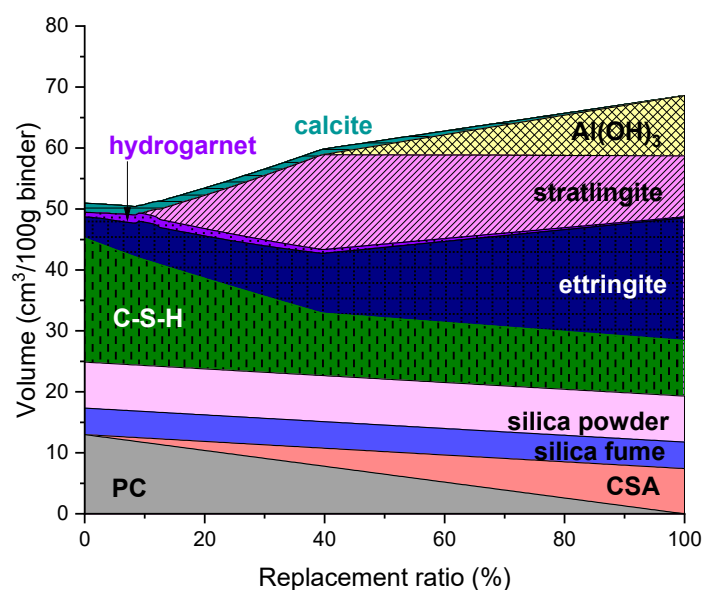


Figure 2. Predicted phase assemblage of UHPC containing CSA.

### 3.3. MK-Containing UHPC

The predicted phase assemblage of UHPC containing MK is shown in Figure 3. Replacing PC with MK in UHPC initially decreased the amount of C-S-H that forms in the mixture. Unlike those containing CSA or CAC, ettringite was found stable up to 25% replacement. In addition, the amount of Fe-hydrogarnet gradually decreased as less PC was used. The formation of  $\text{Al}(\text{OH})_3$  and amorphous silica was initiated at 17% and 31% replacement ratios, respectively. The formation of amorphous silica in MK-containing UHPC indicates that the proportion of  $\text{SiO}_2$  in the mixture can be excessive; thus, replacing MK beyond this ratio (31%) may not be beneficial. The modeling result suggested that gypsum may precipitate at the replacement ratio of 25–90%.

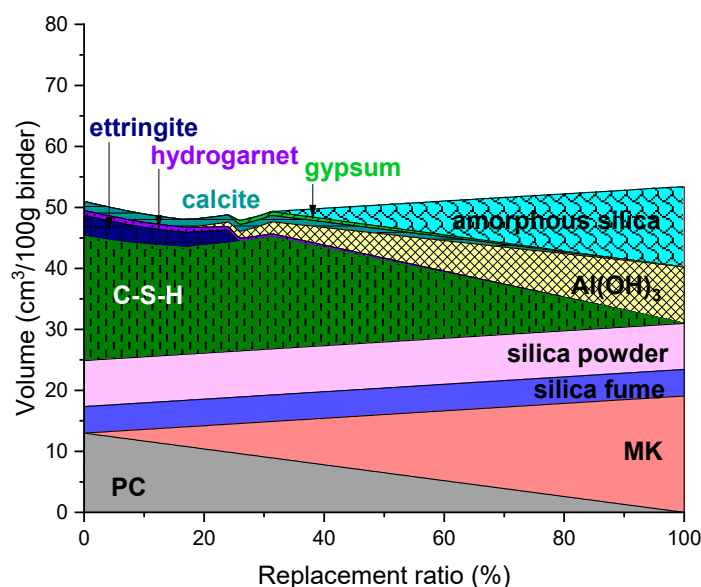


Figure 3. Predicted phase assemblage of UHPC containing MK.

The predicted volume change in the MK-containing UHPC was relatively lower than what was expected for the CSA- and CAC-containing UHPC. The overall solid volume was predicted to gradually decrease up to ~25% replacement and start increasing beyond this replacement level.

### 3.4. BFS-Containing UHPC

The predicted phase assemblage of UHPC containing BFS is shown in Figure 4. It is noticed that replacing PC with BFS brought the fewest changes in the phase assemblage in comparison with the other mixture combinations. Replacing PC with BFS in UHPC resulted in a marginal decrease in the volume of C-S-H and a more notable decrease in ettringite.

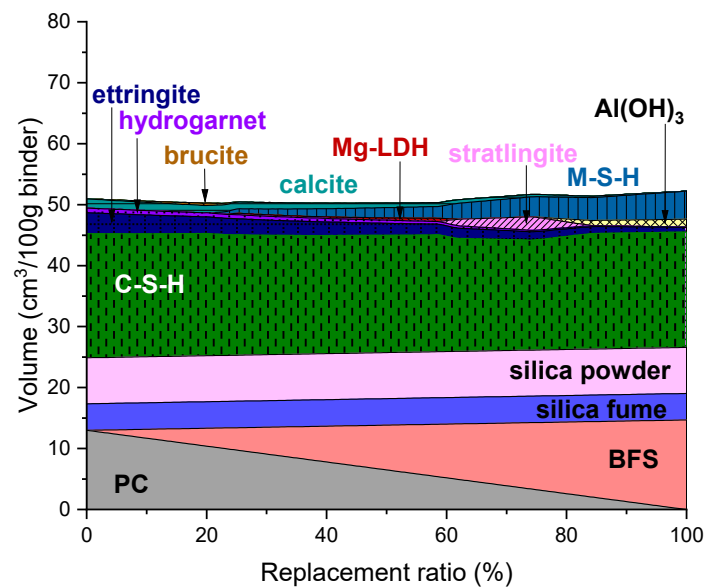


Figure 4. Predicted phase assemblage of UHPC containing BFS.

There were a number of Mg-bearing phases observed in the simulation. Brucite and Mg-LDH were predicted to form as transient phases, which are stable at 1–25% and 23–62% replacement ratios, respectively. These Mg-bearing phases were expected to convert into M-S-H at higher replacement ratios. Strätlingite was found stable at 59–84% replacement and expected to destabilize to Al(OH)<sub>3</sub> and M-S-H at higher replacement levels.

The predicted volume change throughout all replacement ratios was the lowest of the prediction results presented in this work. This may be associated with the phase assemblage in the BFS-containing UHPC, which remains almost unchanged upon replacement of PC.

## 4. Discussion

The thermodynamic modeling results imply that the porosity evolution would vary dramatically according to the cementitious binders that were used to replace PC and their dosages (Figure 5). The prediction results suggest that when the dosage of CAC and CSA is greater than 24 and 12%, respectively, the mixtures are expected to have lower porosity compared to the UHPC solely consisting of PC. Replacing PC with CSA is expected to have the lowest porosity among all simulated mixtures and can induce expansion problems when the replacement ratio exceeds 35%, according to the simulation.

The water demand of the mixtures is simulated in Figure 6 as a function of replacement ratios. Note that the predicted water demand is the amount of water needed for chemical reactions during hydration as predicted by thermodynamic calculations; thus, it is not related to the amount of water needed to ensure homogeneous mixing. The obtained results showed some correlations with the predicted porosity, suggesting that higher water demand leads to generating lower porosity in the matrix. It is advisable that more water is added to the mixtures incorporating CAC or CSA in replacement of PC, because these binders are predicted to consume more water; otherwise, they are known to cause expansion at later ages due to the hydration of anhydrous clinkers at hardened states [26,33,34].

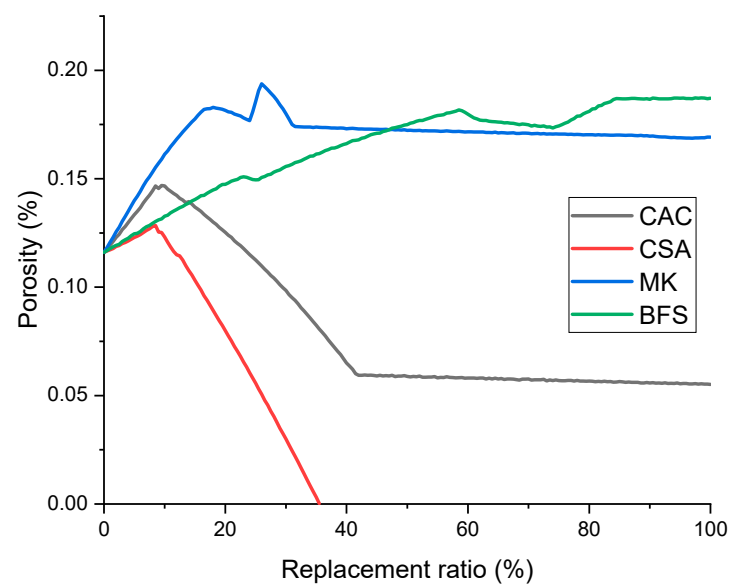


Figure 5. Predicted porosity as a function of replacement ratios.

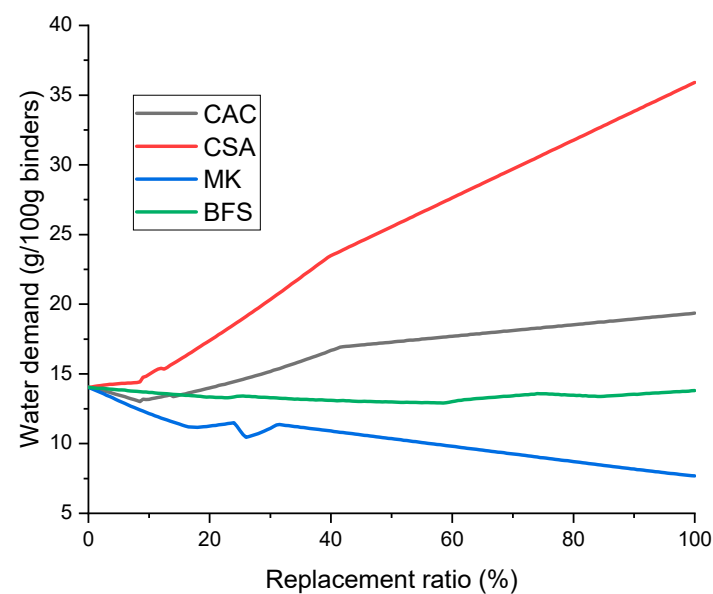


Figure 6. Predicted water demand of UHPC mixtures as a function of replacement ratios.

It is important that the results reported in this work should be cross-checked with the test results before being implemented in practice. The experimental tests for UHPC consisting of alternative cementitious binders will therefore be conducted in forthcoming studies.

## 5. Conclusions

This study investigated the effect of using alternative cementitious binders in UHPC by adopting thermodynamic calculations. Replacing PC in UHPC with CAC, CSA, MK or BFS is expected to result in significant variations in the phase assemblages. The main outcomes of this study can be summarized as follows.

- (1) Strätlingite is predicted as a predominant phase in both CAC- and CSA-containing UHPC. Ettringite would increasingly form as PC is replaced with CSA.
- (2) The volume of C-S-H is expected to notably decrease when replacing PC with MK, while this was not the case with BFS-containing UHPC. C-S-H remained as a predominant phase in BFS-containing UHPC throughout all replacement ratios.

- (3) The predicted water demand per binder mass suggests that more water is needed for chemical reactions when using CSA and CAC, while a similar or lower amount of water is needed when using BFS and MK as a replacement of PC.
- (4) It is expected that use of CSA or CAC would lead to decreasing the porosity in UHPC, while using BFS or MK may increase the porosity in comparison with that solely consisting of PC.

**Author Contributions:** Conceptualization, G.-S.R.; Data curation, S.P., G.-H.A. and K.-T.K.; Formal analysis, S.P., N.L., G.-S.R., G.-H.A. and K.-T.K.; Funding acquisition, G.-S.R.; Investigation, S.P., N.L., G.-S.R., G.-H.A. and K.-T.K.; Methodology, S.P., N.L., G.-S.R., G.-H.A. and K.-T.K.; Project administration, G.-S.R.; Resources, G.-S.R.; Validation, G.-H.A.; Visualization, G.-S.R. and K.-T.K.; Writing—original draft, S.P.; Writing—review and editing, N.L., G.-S.R., G.-H.A. and K.-T.K. All authors have read and agreed to the published version of the manuscript.

**Funding:** This work was financially supported by the Korea Institute of Civil Engineering and Building Technology (project no. 20210120).

**Institutional Review Board Statement:** Not applicable.

**Informed Consent Statement:** Not applicable.

**Data Availability Statement:** The data presented in this study are available on request.

**Conflicts of Interest:** The authors declare no conflict of interest.

## References

1. Shi, C.; Wu, Z.; Xiao, J.; Wang, D.; Huang, Z.; Fang, Z. A review on ultra high performance concrete: Part I—Raw materials and mixture design. *Constr. Build. Mater.* **2015**, *101*, 741–751. [[CrossRef](#)]
2. Du, J.; Meng, W.; Khayat, K.H.; Bao, Y.; Guo, P.; Lyu, Z.; Abu-obeidah, A.; Nassif, H.; Wang, H. New development of ultra-high-performance concrete (UHPC). *Compos. Part B Eng.* **2021**, *224*, 109220. [[CrossRef](#)]
3. Dils, J.; Boel, V.; De Schutter, G. Influence of cement type and mixing pressure on air content, rheology and mechanical properties of UHPC. *Constr. Build. Mater.* **2013**, *41*, 455–463. [[CrossRef](#)]
4. Khayat, K.H.; Meng, W.; Vallurupalli, K.; Teng, L. Rheological properties of ultra-high-performance concrete—An overview. *Cem. Concr. Res.* **2019**, *124*, 105828. [[CrossRef](#)]
5. Choi, M.S.; Lee, J.S.; Ryu, K.S.; Koh, K.-T.; Kwon, S.H. Estimation of rheological properties of UHPC using mini slump test. *Constr. Build. Mater.* **2016**, *106*, 632–639. [[CrossRef](#)]
6. Pyo, S.; Wille, K.; El-Tawil, S.; Naaman, A.E. Strain rate dependent properties of ultra high performance fiber reinforced concrete (UHP-FRC) under tension. *Cem. Concr. Compos.* **2015**, *56*, 15–24. [[CrossRef](#)]
7. Wang, R.; Gao, X.; Huang, H.; Han, G. Influence of rheological properties of cement mortar on steel fiber distribution in UHPC. *Constr. Build. Mater.* **2017**, *144*, 65–73. [[CrossRef](#)]
8. Richard, P.; Cheyrezy, M. Composition of reactive powder concretes. *Cem. Concr. Res.* **1995**, *25*, 1501–1511. [[CrossRef](#)]
9. Kim, H.; Koh, T.; Pyo, S. Enhancing flowability and sustainability of ultra high performance concrete incorporating high replacement levels of industrial slags. *Constr. Build. Mater.* **2016**, *123*, 153–160. [[CrossRef](#)]
10. Pyo, S.; Kim, H.-K.; Lee, B.Y. Effects of coarser fine aggregate on tensile properties of ultra high performance concrete. *Cem. Concr. Compos.* **2017**, *84*, 28–35. [[CrossRef](#)]
11. Pyo, S.; Tafesse, M.; Kim, B.-J.; Kim, H.-K. Effects of quartz-based mine tailings on characteristics and leaching behavior of ultra-high performance concrete. *Constr. Build. Mater.* **2018**, *166*, 110–117. [[CrossRef](#)]
12. Bajaber, M.; Hakeem, I. UHPC evolution, development, and utilization in construction: A review. *J. Mater. Res. Technol.* **2020**, *10*, 1058–1074. [[CrossRef](#)]
13. Xue, J.; Briseghella, B.; Huang, F.; Nuti, C.; Tabatabai, H.; Chen, B. Review of ultra-high performance concrete and its application in bridge engineering. *Constr. Build. Mater.* **2020**, *260*, 119844. [[CrossRef](#)]
14. Bae, Y.; Pyo, S. Ultra high performance concrete (UHPC) sleeper: Structural design and performance. *Eng. Struct.* **2020**, *210*, 110374. [[CrossRef](#)]
15. Bae, Y.; Pyo, S. Effect of steel fiber content on structural and electrical properties of ultra high performance concrete (UHPC) sleepers. *Eng. Struct.* **2020**, *222*, 111131. [[CrossRef](#)]
16. Song, M.; Wang, C.; Cui, Y.; Li, Q.; Gao, Z. Mechanical Performance and Microstructure of Ultra-High-Performance Concrete Modified by Calcium Sulfoaluminate Cement. *Adv. Civ. Eng.* **2021**, *2021*, 4002536. [[CrossRef](#)]
17. Lee, N.; Koh, K.; Park, S.; Ryu, G. Microstructural investigation of calcium aluminate cement-based ultra-high performance concrete (UHPC) exposed to high temperatures. *Cem. Concr. Res.* **2017**, *102*, 109–118. [[CrossRef](#)]

18. Pyo, S.; Kim, H.-K. Fresh and hardened properties of ultra-high performance concrete incorporating coal bottom ash and slag powder. *Constr. Build. Mater.* **2017**, *131*, 459–466. [[CrossRef](#)]
19. Peng, Y.Z.; Huang, J.; Ke, J. Preparation of ultra-high performance concrete using phosphorous slag powder. *Appl. Mech. Mater.* **2013**, *357–360*, 588–591. [[CrossRef](#)]
20. He, Z.-H.; Du, S.-G.; Chen, D. Microstructure of ultra high performance concrete containing lithium slag. *J. Hazard. Mater.* **2018**, *353*, 35–43. [[CrossRef](#)] [[PubMed](#)]
21. Abdulkareem, O.M.; Fraj, A.B.; Bouasker, M.; Khouchaf, L.; Khelidj, A. Microstructural investigation of slag-blended UHPC: The effects of slag content and chemical/thermal activation. *Constr. Build. Mater.* **2021**, *292*, 123455. [[CrossRef](#)]
22. Rangaraju, P.R.; Li, Z. Development of UHPC Using Ternary Blends of Ultra-Fine Class F Fly Ash, Meta-kaolin and Portland Cement. In Proceedings of the First International Interactive Symposium on Ultra-High Performance Concrete, Des Moines, IA, USA, 18–20 July 2016.
23. Norhasri, M.M.; Hamidah, M.; Fadzil, A.M.; Megawati, O. Inclusion of nano metakaolin as additive in ultra high performance concrete (UHPC). *Constr. Build. Mater.* **2016**, *127*, 167–175. [[CrossRef](#)]
24. He, Z.-H.; Zhu, H.-N.; Zhang, M.-Y.; Shi, J.-Y.; Du, S.-G.; Liu, B. Autogenous shrinkage and nano-mechanical properties of UHPC containing waste brick powder derived from construction and demolition waste. *Constr. Build. Mater.* **2021**, *306*, 124869. [[CrossRef](#)]
25. Park, S.; Wu, S.; Liu, Z.; Pyo, S. The role of supplementary cementitious materials (SCMs) in ultra high performance concrete (UHPC): A review. *Materials* **2021**, *14*, 1472. [[CrossRef](#)] [[PubMed](#)]
26. Park, S.; Jeong, Y.; Moon, J.; Lee, N. Hydration characteristics of calcium sulfoaluminate (CSA) cement/Portland cement blended pastes. *J. Build. Eng.* **2020**, *34*, 101880. [[CrossRef](#)]
27. Bizzozero, J.; Scrivener, K.L. Limestone reaction in calcium aluminate cement–calcium sulfate systems. *Cem. Concr. Res.* **2015**, *76*, 159–169. [[CrossRef](#)]
28. Avet, F.; Li, X.; Scrivener, K. Determination of the amount of reacted metakaolin in calcined clay blends. *Cem. Concr. Res.* **2018**, *106*, 40–48. [[CrossRef](#)]
29. Kocaba, V.; Gallucci, E.; Scrivener, K.L. Methods for determination of degree of reaction of slag in blended cement pastes. *Cem. Concr. Res.* **2012**, *42*, 511–525. [[CrossRef](#)]
30. Kulik, D.; Berner, U.; Curti, E. *Modelling Chemical Equilibrium Partitioning with the GEMS-PSI Code*; Paul Scherrer Institute: Villigen, Switzerland, 2004.
31. Kulik, D.A.; Wagner, T.; Dmytrieva, S.V.; Kosakowski, G.; Hingerl, F.F.; Chudnenko, K.V.; Berner, U.R. GEM-Selektor geochemical modeling package: Revised algorithm and GEMS3K numerical kernel for coupled simulation codes. *Comput. Geosci.* **2013**, *17*, 1–24. [[CrossRef](#)]
32. Lothenbach, B.; Kulik, D.A.; Matschei, T.; Balonis, M.; Baquerizo, L.; Dilnesa, B.; Miron, G.D.; Myers, R.J. Cemdata18: A chemical thermodynamic database for hydrated Portland cements and alkali-activated materials. *Cem. Concr. Res.* **2019**, *115*, 472–506. [[CrossRef](#)]
33. Sorensen, A.; Thomas, R.; Maguire, M.; Quezada, I. Calcium Sulfoaluminate (CSA) Cement: Benefits and Applications. *Concr. Int.* **2018**, *40*, 65–69.
34. Singh, B.K.; Hafeez, M.A.; Kim, H.; Hong, S.; Kang, J.; Um, W. Inorganic waste forms for efficient immobilization of radionuclides. *ACS EST Eng.* **2021**, *1*, 1149–1170. [[CrossRef](#)]